

# On the detection of caustic crossing events associated with dark matter in the form of primordial black holes

M. R. S. Hawkins<sup>1</sup>★

<sup>1</sup>*Institute for Astronomy (IfA), University of Edinburgh, Royal Observatory, Blackford Hill, Edinburgh EH9 3HJ, UK*

Accepted XXX. Received YYY; in original form ZZZ

## ABSTRACT

The possibility that stellar mass primordial black holes may make up at least a significant fraction of dark matter has recently received much attention, partly as a result of gravitational wave observations, but more specifically from observations of microlensing in the Galactic halo and in quasar gravitational lens systems. If this is the case then a number of observable consequences are to be expected. This paper focusses on the prediction that dark matter in the form of primordial black holes will result in a web of caustics which when traversed by quasars will result in a complex but characteristic amplification of the accretion disc light source. Caustic crossings produce features in quasar light curves which are relatively straightforward to identify, and are hard to associate with any intrinsic mode of variation. Microlensing simulations are used to clarify the nature of the expected light curve features, and compared with observed light curves to demonstrate that caustic crossing features can be present. A further test of microlensing is based on the expected statistical symmetry of the light curves, which is not predicted for most models of intrinsic quasar variability, but is found in large samples of quasar light curves. The conclusion of the paper is that observations of quasar light curves are consistent with the expected microlensing amplifications from dark matter made up of stellar mass primordial black holes, but cannot easily be explained by intrinsic variations of the quasar accretion disc.

**Key words:** quasars: general – gravitational lensing: micro – dark matter

## 1 INTRODUCTION

The idea that dark matter may be in the form of primordial black holes, or perhaps other compact bodies, has received considerable observational support in the last few years (Carr et al. 2024). The main obstacle to the identification of compact bodies as dark matter over the last 50 years or so has been the widely accepted view that dark matter is in the form of non-baryonic elementary particles. The reason for the acceptance of this paradigm is not entirely clear, as attempts to detect plausible dark matter particles have consistently failed over this period. As the limitation of the neutrino floor or ‘fog’ (O’Hare 2021) is approached by dark matter particle detectors, the prospects for direct detection do not look good, and there now seems to be a paradigm shift towards primordial black holes as dark matter.

If indeed dark matter is in the form of primordial black holes, then the associated mass function is expected to be very broad, but with some well defined peaks in probability, notably associated with phase transitions (Carr et al. 2021). Of particular interest is the peak associated with the QCD phase transition (Byrnes et al. 2018) where the most probable mass for a primordial black hole is around  $0.7M_{\odot}$ . If a significant fraction of dark matter is indeed in the form of solar mass primordial black holes, then there are a number of cosmological situations where they would be expected to betray their presence in a detectable way.

The first large scale programme to detect dark matter in the form

of compact bodies (Alcock et al. 1996, 2000) involved monitoring several million stars in the Magellanic Clouds to look for evidence of microlensing by compact bodies in the Galactic halo. The results implied the detection of a large halo population of stellar mass compact bodies which could not be accounted for by any known stellar population. This raised the question of whether these objects could make up the dark matter. On the assumption of a flat halo rotation curve and a relatively narrow mass function, the authors concluded that less than 40% of the halo could be made up of compact bodies (Alcock et al. 2000). However, it is now clear that the Milky Way rotation curve is not flat (Hawkins 2015; Calcino et al. 2018), but declines implying a reduced dark matter content which is consistent with the compact bodies detected by the MACHO project making up the dark matter. Recently, the decline of the Milky Way rotation speed has been confirmed beyond reasonable doubt (Jiao et al. 2023; Ou et al. 2024; García-Bellido & Hawkins 2024) by observations from the *Gaia* DR3 data release<sup>1</sup>.

The detection of a compact body component of dark matter in the Milky Way halo was followed by investigations into the make-up of more distant galaxy halos. In particular, gravitational lens systems have provided a very useful environment for detecting compact bodies in galaxy halos. It is well-known that as well as varying in response to changes in quasar luminosity, individual images vary independently, often by large amounts (Mediavilla et al. 2009; Pooley et al. 2012; Bate et al. 2018). These changes have been widely attributed

★ E-mail: mrsh@roe.ac.uk

<sup>1</sup> <https://www.cosmos.esa.int/web/gaia/dr3>

to microlensing by compact bodies in the halo of the lensing galaxy, but there has been some debate as to whether the lenses are halo stars, or compact bodies making up the halo dark matter (Hawkins 2020a). The question now seems to be settled by observations of the cluster lens SDSS J1004+4112 where strong microlensing amplifications are observed some 60 kpc from the cluster centre, far beyond the distribution of stars which declines to a negligible level beyond 25 kpc (Hawkins 2020b). If a significant fraction of dark matter is indeed in the form of compact bodies, then there are a number of other situations where one might expect them to betray their presence.

An early observation that the expected time dilation in quasar light curves due to intrinsic variations was not observed (Hawkins 2010) led to the proposal that apparent changes in quasar luminosity were more plausibly attributed to microlensing amplifications, where the detection of time dilation would not be expected. Recently however it has been shown (Lewis & Brewer 2023) that time dilation is seen in quasars, implying that any time dilation signal from intrinsic variations can still be detected. This is consistent with recent work (Hawkins 2022) showing that to reproduce the observed distribution of quasar amplitudes of variation it is necessary to include both intrinsic variations and microlensing amplifications from a cosmic distribution of stellar mass compact bodies.

In addition to amplifying the light from the quasar nucleus, there is a strong case that knots in a turbulent broad line region will also be microlensed, leading to rapid changes in the shape and structure of quasar broad emission lines (Hawkins 2024). This has been observed in a number of quasar spectra, where new components of broad emission lines appear or disappear on a timescale of a few years, an order of magnitude shorter than the dynamic timescale of the broad line region (Peterson 1993). This is best explained by rapid microlensing amplification of knots in the broad line region with radial velocities differing by several hundred km sec<sup>-1</sup> from the systemic velocity, and is consistent with expectations for a population of primordial black holes making up the dark matter.

There have been many attempts over the years to find evidence for microlensing, and hence a population of compact bodies, by examining the properties of quasar light curves. The main difficulty with this approach has always been to distinguish microlensing from intrinsic variation. In their classic book on Gravitational Lenses, Schneider et al. (1992) point out that, "It is very difficult to separate the intrinsic variability of a source from lensing effects; the only hope is to find features in the light curve characteristic of microlensing events". This is largely the motivation for the present work.

In this paper, an additional expected consequence of dark matter made up of stellar mass compact bodies is examined. At a sufficiently high redshift the optical depth to microlensing  $\tau$  will be large enough for caustic webs to form in the amplification pattern of the lenses. This will result in distinctive cusp-like features to be present in the microlensing light curves. The identification of such features provides a necessary consistency check for the hypothesis that the dark matter is made up of compact bodies. It is the purpose of this paper to look for such events.

The structure of the paper is as follows. Section 2 describes the quasar monitoring programmes which were used to identify candidate caustic crossing features, and computer simulations to produce templates for identifications. Section 3 gives examples of more realistic computer simulations to be compared with observed features in quasar light curves, and discusses the processes which produce them. Section 4 shows candidate caustic crossing events and relates them to simulated microlensing events, as well as giving some light curve statistics relevant to microlensing. The final sections are for Discussion and Conclusions.

## 2 DATA

This section is devoted to a description of the quasar monitoring programmes which form the basis for the search for microlensing events, and a description of the microlensing simulations which have been used as templates for identifying caustic crossing events.

### 2.1 Observations of quasar light curves

Since the first observations of quasar optical variability (Matthews & Sandage 1963), there have been a number of multicolour monitoring programmes, pioneered by Giveon et al. (1999) with a sample of 42 nearby quasars observed for 7 years. This work was followed by a larger photographic survey (Hawkins 1996, 2007) in which some 1000 quasars were monitored for a period of 26 years, with data held in the SuperCOSMOS Science Archive (SSA)<sup>2</sup> and more recently the SDSS Legacy Survey (MacLeod et al. 2012) in Stripe 82<sup>3</sup> with light curves for nearly 10,000 quasars covering up to 8 years. These surveys were designed to understand the nature of the observed variations in quasar light, and form an excellent basis for the search for caustic crossing events.

The first survey large enough to be useful for detecting microlensing events was the photographic monitoring programme (Hawkins 1996, 2007) undertaken with the UK 1.2 Schmidt telescope at Siding Springs Observatory, Australia, in ESO/SERC Field 287 centred on 21<sup>h</sup>28<sup>m</sup>, -45° (1950). The plates were digitised by the SuperCOSMOS measuring machine at the Royal Observatory, Edinburgh (Hambly et al. 2001) to give calibrated magnitudes for the several hundred thousand images on the 6° x 6° plates. In a recent update of the survey (Hawkins 2022), the catalogue now contains some 1033 quasar light curves in the  $B_J$  (close to  $g$ ) and  $R$  passbands, with yearly mean magnitudes for 26 years from 1977 to 2002 and photometric errors < 0.04 magnitudes.

### 2.2 Microlensing simulations

The unambiguous detection of microlensing events in quasar light curves presents a number of challenges, mostly connected with the difficulty of distinguishing between intrinsic variations in the quasar luminosity as opposed to amplification of the accretion disc by microlensing events. A number of factors will contribute to the likelihood of microlensing events being detected, including the redshift of the quasar, the crowdedness of the population of lenses, the dimensions and structure of the quasar accretion disc, the size of the sample of quasars, and the length of time for which the quasars are monitored.

The particular focus of this paper is to look for evidence of microlensing amplification by a population of compact bodies, which must be distinguished from changes in the luminosity of the quasar accretion disc. For isolated lenses, microlensing amplification will take the form of a characteristic bell-shaped profile (Paczynski 1986; Alcock et al. 1996), commonly referred to as a Paczynski profile, with source amplification  $A$  given by

$$A = \frac{u^2 + 2}{u\sqrt{u^2 + 4}} \quad (1)$$

where  $u = b/R_E$  is the impact parameter, and  $b$  and  $R_E$  are the

<sup>2</sup> <http://ssa.roe.ac.uk>

<sup>3</sup> <https://faculty.washington.edu/ivezic/macLeod/qso-dr7/Southern.html>

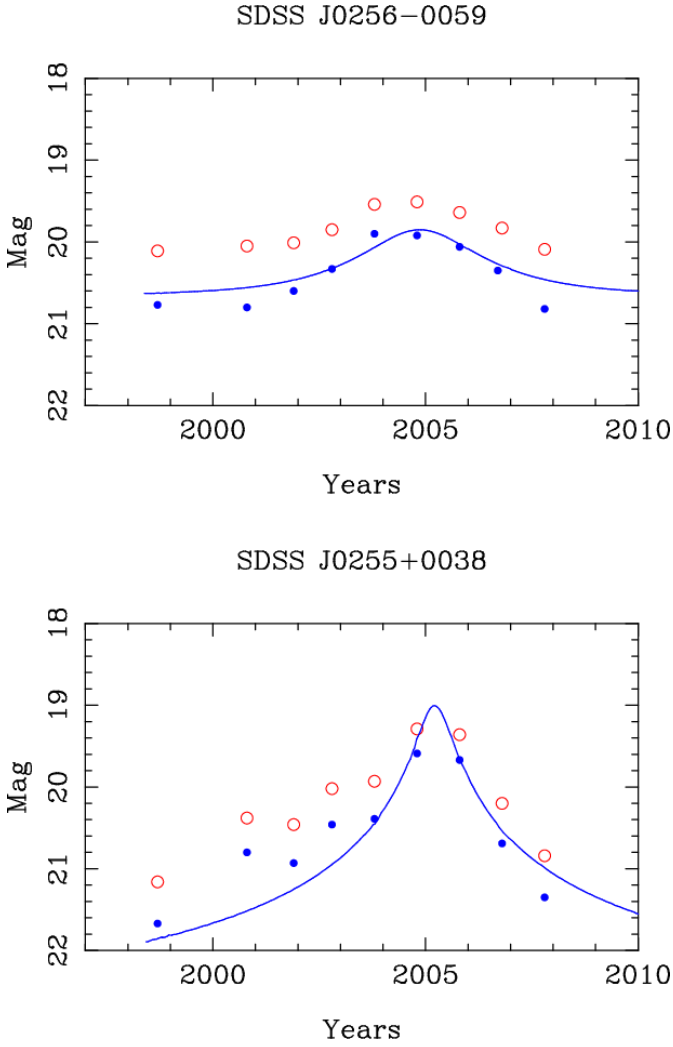


**Figure 1.** Examples of candidate microlensing events from Luo et al. (2020). Blue filled and red open circles show average yearly magnitudes for the  $g$  and  $r$  band filters respectively. The continuous blue line shows a Paczyński profile (Alcock et al. 1996) fitted to the  $g$ -band data.

separation of the lens from the line of sight to the quasar and the Einstein radius of the lens respectively. However, when a source is amplified by two lenses, the amplification patterns combine in a non-linear way to produce astroid like features, well illustrated for the case of a two-point-mass lens by Schneider & Weiss (1986). As the value of  $\tau$  increases, complex magnification patterns dominated by astroid-like caustics emerge. The transition from the low optical depth regime is estimated to occur for a value of  $\tau$  of around 0.1 (Kofman et al. 1997), which for dark matter in the form of compact bodies in a  $\Lambda$ CDM cosmology implies a redshift for the quasar of  $z \sim 1.3$  (Fukugita et al. 1992). It is therefore to be expected that in a large sample of quasars with say  $z > 1.5$ , occasional caustic crossing events may be observed in quasar light curves.

In a recent paper (Luo et al. 2020) largely devoted to characterising the optical light curves of extreme variability quasars, the authors also identify a sample of 16 quasars with bell shaped light curves which they present as candidate microlensing events. The main database for their search is the SDSS Legacy photometric monitoring programme

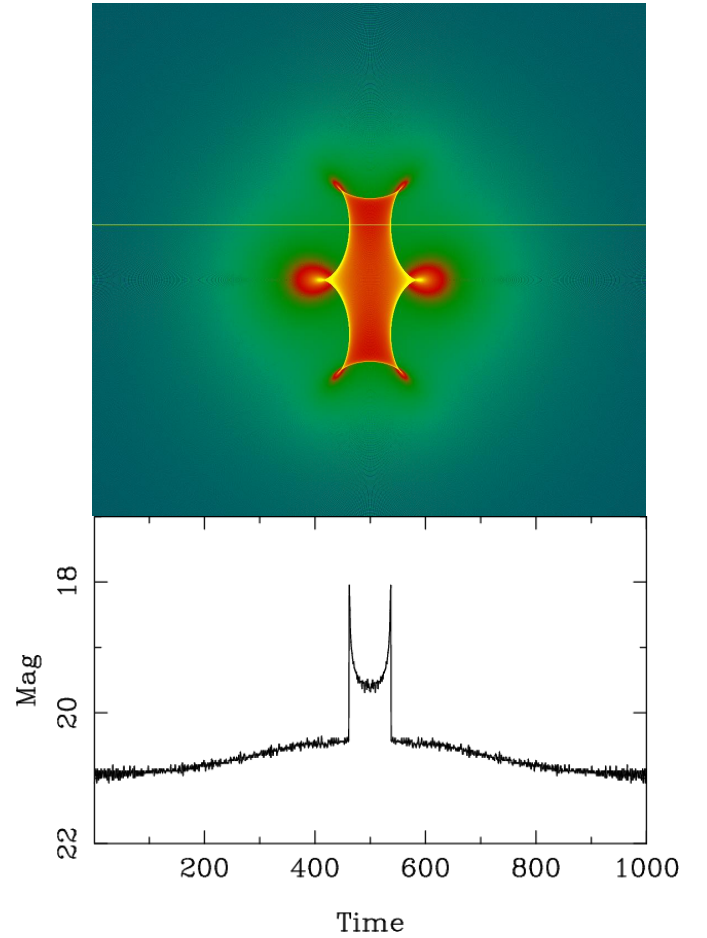


**Figure 2.** Microlensing magnification pattern for two equal mass lenses separated by  $1.0R_E$ , in arbitrary units of time and magnitude. The plot shows critical curves similar to those for the analytic solution illustrated in Figure 2 of Schneider & Weiss (1986). The bottom panel shows the light curve traced out by the yellow horizontal line, and indicates the magnitude scale.

in Stripe 82, with additional measures to extend the light curves from the Pan-STARRS1 data archive<sup>4</sup> and the Dark Energy Survey<sup>5</sup>. Two examples of light curves from the list of microlensing candidates identified by Luo et al. (2020) are plotted in Fig. 1. To clarify the trend of the data, the original measurements have been averaged into yearly bins, and for comparison a Paczyński profile has been fitted to the  $g$ -band data.

Although these quasar light curves are certainly plausible candidates for microlensing events, the shape alone is not sufficient for an unambiguous classification as a Paczyński profile from Eq. 1. When two or more lenses lie close to the line of sight to a quasar, within say one Einstein radius, the lenses combine in a non-linear way to produce an astroid-like magnification pattern with clearly defined critical curves. The light curves resulting from the transit of a source across such a complex magnification pattern are not in general susceptible to analytic description, and must be modelled by computer simulation. To achieve this, the ray tracing software of Wambsganss (1999) has been used to simulate the non-linear magnification pattern

<sup>4</sup> <https://catalogs.mast.stsci.edu/panstarrs/>

<sup>5</sup> <https://des.ncsa.illinois.edu/releases/dr2>

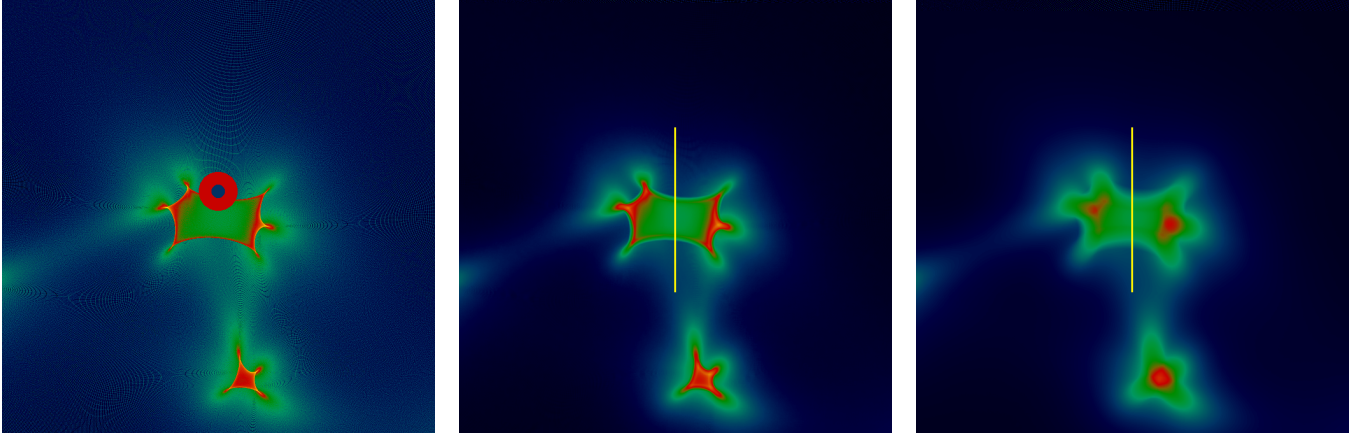


**Figure 3.** Microlensing magnification patterns in arbitrary units of magnitude for a population of  $0.8 M_{\odot}$  bodies with parameter values  $\kappa_* = 0.1$ ,  $\kappa_c = 0$ , and  $\gamma = 0$ . The frames consist of  $680^2$  pixels and have a side length of approximately 5.5 Einstein radii. The left hand panel is for a point source, and the centre and right hand panels assume a uniform disc for the source with radius 1 and 3 lt-day respectively. Assuming redshifts  $z = 0.5$  and  $z = 2.0$  for lens and source, this corresponds to radii 0.06 and  $0.17 R_E$  respectively. To give an idea of relative sizes, in the left hand panel discs with radii 1 and 3 lt-day are superimposed on the caustic pattern. The yellow lines indicate the trajectory of a quasar across the amplification pattern during a caustic crossing event, and the resulting light curves are plotted in Fig. 4, and indicate the magnitude scale. The zeropoint of the colour code is arbitrary.

resulting from multiple lens configurations. In these situations, the resulting light curves show characteristic cusp-like features which are far more readily identified as microlensing features than Paczyński profiles.

### 3 METHODS

The first step up in complexity from the single lens Paczyński profile is the case of two equal mass lenses, which has in fact been treated analytically by [Schneider & Weiss \(1986\)](#), who trace out the critical curves for a range of lens separations. As an example, the ray tracing software of [Wambsganss \(1999\)](#) has been used to simulate the magnification pattern for two equal mass lenses separated by  $1.0 R_E$ , illustrated in the top panel of Fig. 2. The bottom panel shows the light curve corresponding to the simulated amplification pattern where the crossing of the critical curves can be seen as sharp cusps. Examples of light curves where these characteristic cusps are clearly defined are well illustrated by simulations from [Refsdal & Stabell \(1991\)](#). In a search for examples of microlensing events, these cusp like features are far more distinctive and unambiguous than the bell shape of a Paczyński profile as illustrated in Fig. 1.

The amplification pattern in Fig. 2 assumes a point source. In more realistic cosmological simulations ([Hawkins 2020a, 2022](#)), the source size in the form of the quasar accretion disc will not necessarily be negligible compared with the Einstein radius of the lenses. To illustrate the effect of a finite source size, Fig. 3 shows a cut-out of caustic features from a large area simulation with surface density  $\kappa_*$  in compact bodies or lenses, where  $\kappa_* = 0.1$ . The timescale for the simulation is set by assuming a stellar mass lens, typical values for the source and lens redshifts, and the conventionally adopted value of  $600 \text{ km sec}^{-1}$  for the net transverse velocity ([Kayser et al. 1986](#)), recently refined by [Neira et al. \(2020\)](#) for specific quasar systems. The three panels show amplification patterns for a point source, and for source sizes 1 and 3 lt-day. To give an idea of relative sizes, in the left hand panel discs corresponding in radius to 1 and 3 lt-day

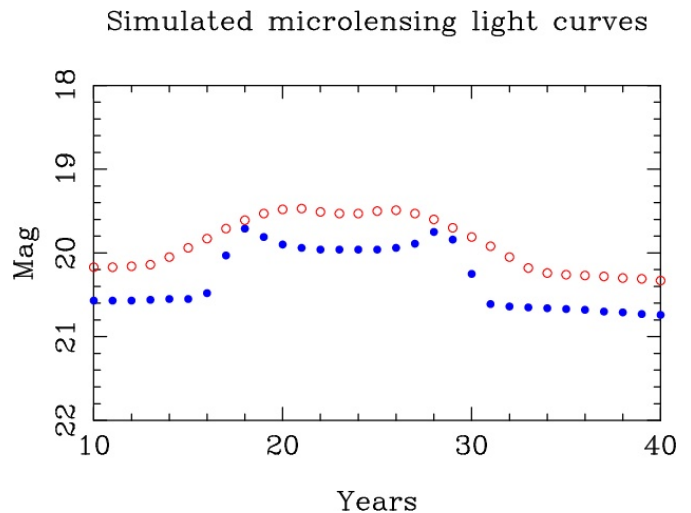


**Figure 4.** Simulated light curves corresponding to the yellow tracks in Fig. 3. The tracks have been plotted as yearly bins to facilitate comparison with observations. The blue filled circles are for a source size of 1 lt-day and the red open circles for 3 lt-day. The magnitude scale has an arbitrary zeropoint.

are superimposed on the caustic pattern. In order to understand the effect that increasing the source size will have on changes in the the observed brightness of a quasar traversing the caustic along the superimposed yellow track in Fig. 3, the resulting light curves are plotted in Fig. 4. The data points show average yearly magnitudes to facilitate comparison with observed light curves. Closed and open circles show light curves for 1 and 3 lt-day quasar accretion disc sizes respectively.

An important feature of microlensing light curves is statistical symmetry, which can be used as a way to distinguish microlensing from intrinsic variations. As [Schneider et al. \(1992\)](#) point out,



"microlensing should yield light curves which are *statistically* symmetric". On a cosmological scale, the assumption of the isotropy of the Universe combined with the geometric nature of the lens equations with no time components implies that microlensing light curves will have no arrow of time. In other words, no statistical test will be able to determine the direction of the time coordinate. In practice this means that for a large sample of quasars, monitored over a sufficiently long period of time, then for any specific change in yearly magnitude, the numbers of increase and decrease in brightness will be equal. This can be used as a way of testing the consistency of microlensing as a significant component of quasar variability.

#### 4 RESULTS

The search for evidence of microlensing in quasar light curves is greatly facilitated if the target events are caustic crossings as simulated in Figs 2 and 4. In this case the expected features are far more distinctive and recognizable than the bell-shaped Paczyński profiles in Fig. 1. Apart from the characteristic cusp-like features of caustic crossings, the radial structure of the quasar accretion disc can provide another parameter for identifying microlensing events (Vernados et al. 2024). A fundamental property of accretion discs is a radial temperature gradient as the disc cools with distance from the central black hole. If significant emission from an area of the accretion disc lies within the Einstein radius of a microlens, then the accretion disc will act as a point source and any amplification due to microlensing will be achromatic. However, in the case where the accretion disc is comparable in size with the Einstein radius of the lens, it will be effectively 'resolved', with the bluer light near the centre acting as a more compact source than the more diffuse red light. This will result in an observable and characteristic difference between the blue and red passband microlensing light curves. This expected pattern is illustrated in Fig. 4, where observations through a blue filter would be represented by the filled circles, and those through a red filter by the open circles. As one might expect, the relatively sharp cusps of the caustic crossing in the blue are smoothed out in the red. This provides another discriminant in searching for caustic crossing candidates in samples of quasar light curves, where such a distinctive pattern of variation is unlikely to be produced at random.

The idea behind this paper is to look for evidence of microlensing amplification as opposed to changes in the luminosity of the quasar accretion disc. In the event that there is a significant temperature gradient across the accretion disc, from a hot blue core in the centre to cool red outer parts, changes in luminosity typically manifest themselves as flares originating in the blue core and propagating outwards to the redder parts of the outer disc, which responds later and less violently than the blue core. This is illustrated in Fig. 5 which shows blue and red passband light curves from the Field 287 survey for a Seyfert galaxy, illustrating the expected features for a brightening of the nuclear accretion disc. The rapid brightening of the blue light which dominates the hot centre is accompanied by a more gradual increase in red light. However, a typical caustic crossing microlensing event has a completely different light curve structure. This is illustrated in Fig. 6, which shows another light curve from the Field 287 survey. In this case the light curve bears a strong resemblance to the caustic crossing simulation in Fig. 4. The overall structure is symmetrical in time, with the blue passband showing cusp-like features which are smoothed out in the red. As discussed in relation to the simulation, this is the result of the compact blue centre of the accretion disc acting as a point source, whereas the more extended redder region is effectively resolved by the microlens.

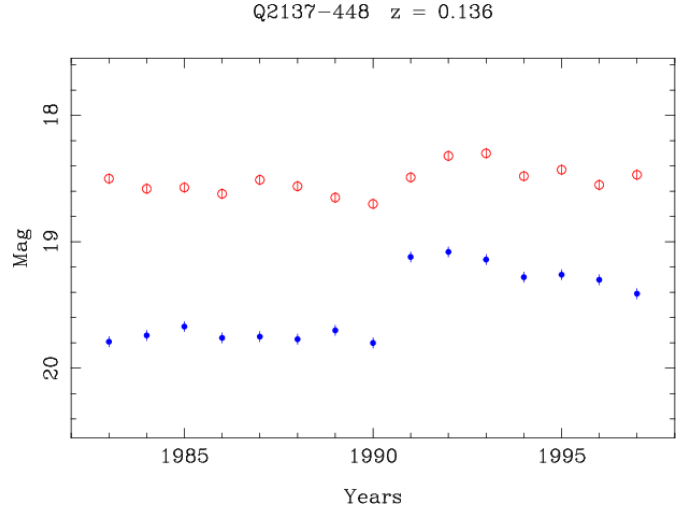


**Figure 5.** Light curve for a low redshift Seyfert galaxy from the Field 287 survey. Filled blue and open red circles show magnitudes for the  $B_J$  and  $R$  passbands respectively. Photometric errors as derived from the data are also plotted.

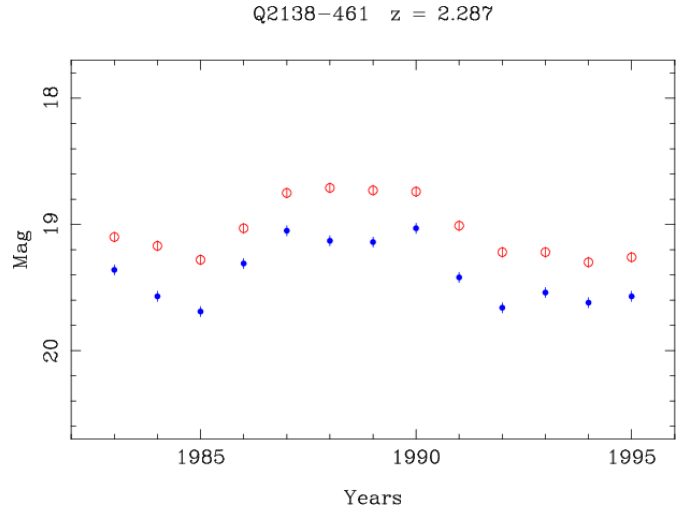


**Figure 6.** Light curve from the Field 287 survey showing a candidate caustic crossing event similar to the simulation in Fig. 4. Symbols are as defined for Fig. 5.

Features similar to those seen in Fig. 6 regularly occur in samples of quasar light curves. The Stripe 82 sample from the SDSS Legacy catalogue of quasar light curves contains many examples, two of which are shown in Fig. 7. Although the addition of extra photometric passbands to the light curves adds some useful definition to the nature of the variations, the shortness of the monitoring period of around 8 years makes it difficult to identify features unambiguously. This is somewhat mitigated by extra epochs from the Pan-STARRS1 data archive, but the inevitable gaps in the observations make for difficulties in identifying features in the light curves.

In general, caustic structures are more complex than those associated with the binary lens in Fig. 2, as may be seen in microlensing simulations with a higher surface density of lenses  $\kappa_*$ , possibly amplified by a smooth distribution of matter  $\kappa_c$ . A typical example

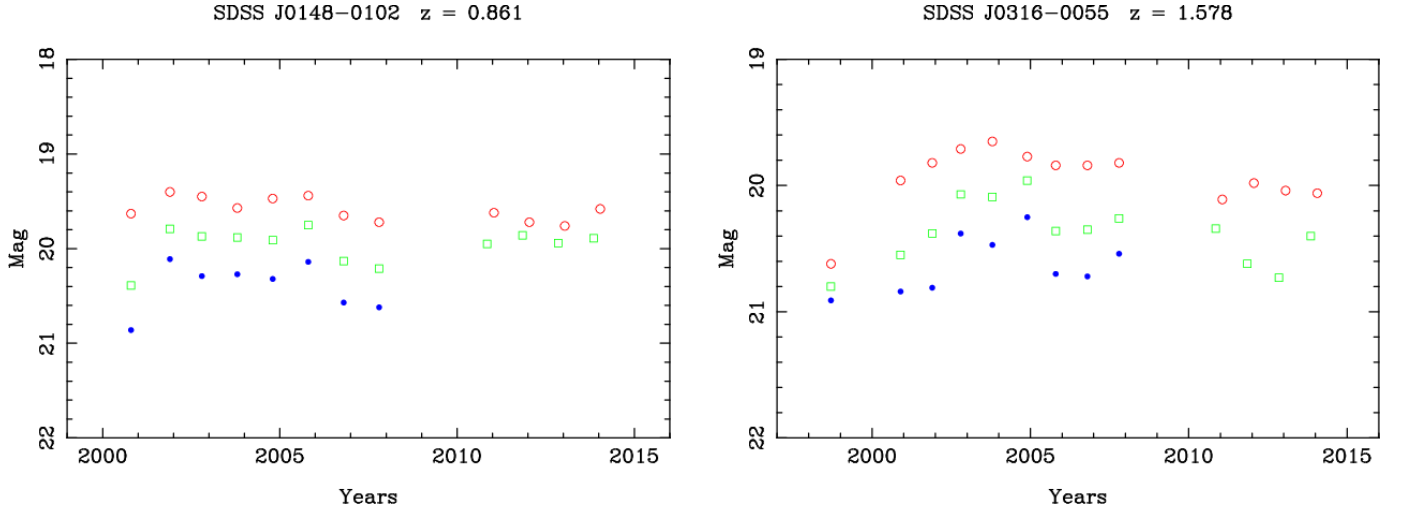


**Figure 7.** Quasar light curves from the SDSS Stripe 82 sample, showing candidate caustic crossing events. Data for the years 1998–2008 are from the SDSS Stripe 82 data archive, and for 2010–2014 from the Pan-STARRS1 data archive. Filled blue circles, open green squares and open red circles show magnitudes for the  $u$ ,  $g$  and  $z$  passbands respectively. The photometric error bars are smaller than the symbols.

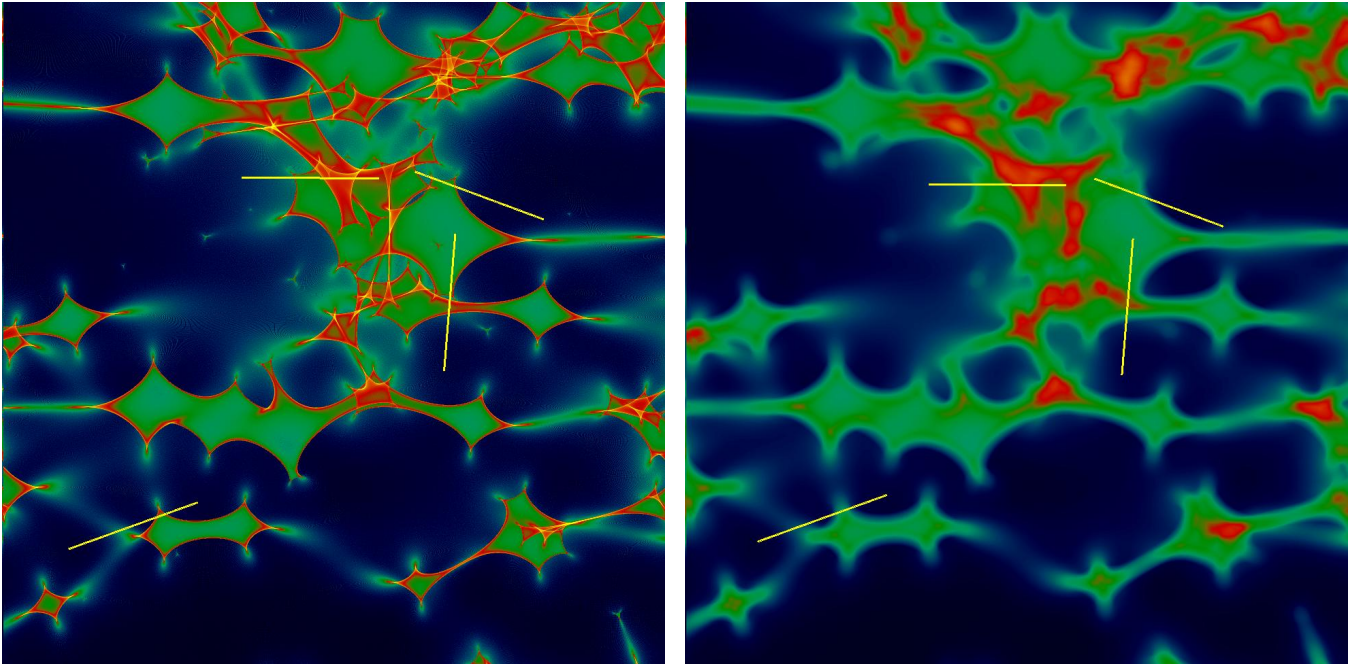


**Figure 8.** Microlensing magnification patterns for a population of  $0.2 M_{\odot}$  bodies with parameter values  $\kappa_* = 0.4$ ,  $\kappa_c = 0$ ,  $\gamma = 0.4$ . The frames consist of  $1000^2$  pixels and have a side length of 8 Einstein radii. The left hand panel is for a point source, and the right hand panel for a source size 2 lt-day, corresponding to  $0.23 R_E$ . The yellow lines represent random 20 year tracks across the caustic pattern.

is shown in Fig. 8, from a simulation using the microlensing code of Wambsganss (1999). The left hand panel shows an amplification pattern for a distribution of point sources with an optical depth to microlensing  $\tau \approx 0.4$ . The right hand panel shows the effect of increasing the source size, or in a cosmological situation the effective radius of the quasar accretion disc. The effect is to blur out the sharp features associated with a point source. To give an idea of how this

might affect the structure of quasar light curves, 4 yellow lines have been superimposed on the simulation, representing random tracks of 20 years duration across the amplification pattern, as might be observed for the light curve of a quasar in a cosmological setting. The 4 light curves corresponding to the yellow tracks are plotted in Fig. 9, where the effect of increasing the source size is clearly illustrated.

In contrast to the light curve for a binary lens as illustrated in Fig. 2

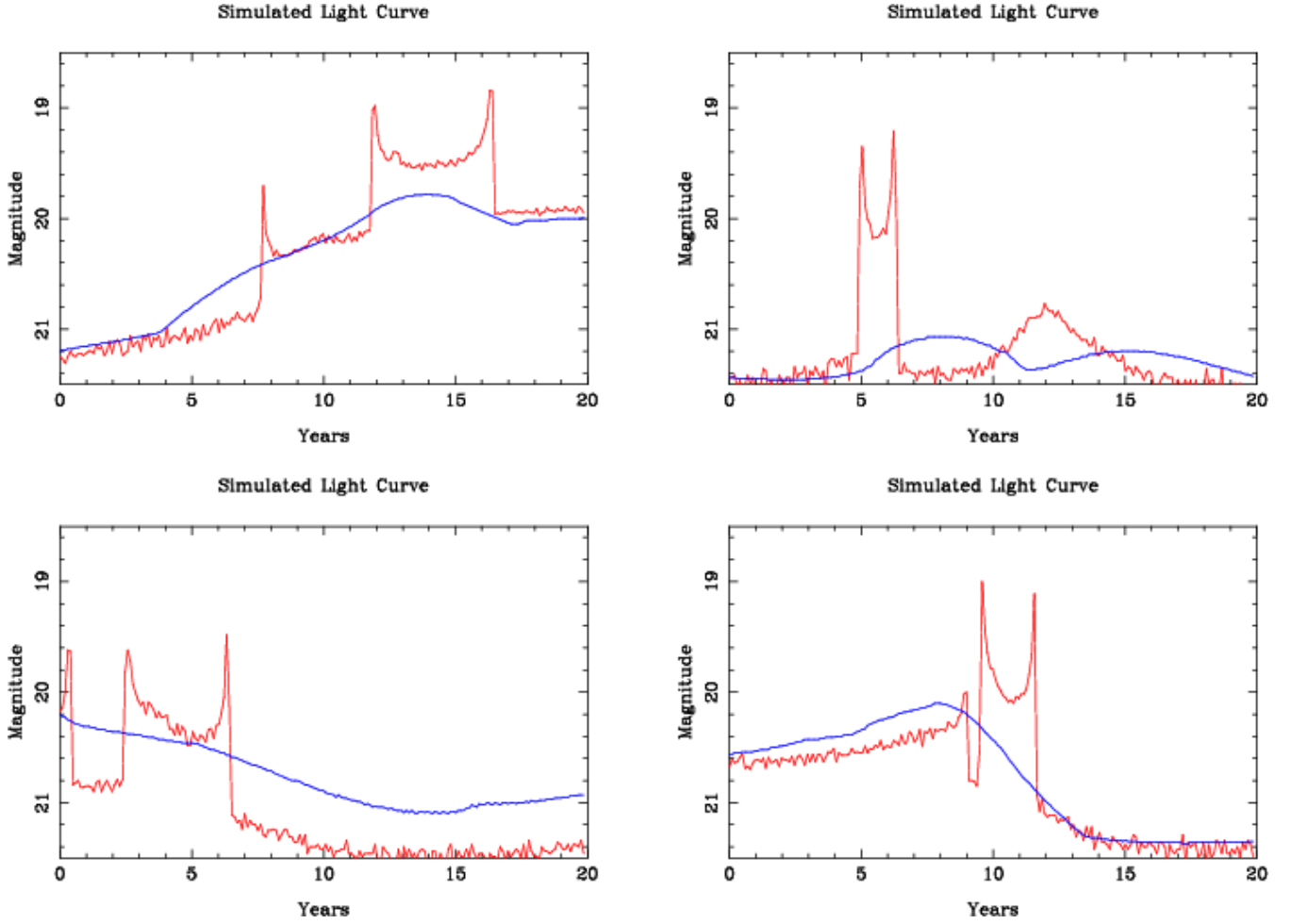


**Figure 9.** Simulated light curves corresponding to the yellow tracks in Fig. 8. The red lines are for a point source (left hand panel Fig. 8), and the blue lines are for a source size of 2 lt-day (right hand panel Fig. 8).

which is well-defined mathematically, or a simple caustic crossing as simulated in Fig. 4, there is clearly a random element to the light curve of a quasar traversing the amplification pattern in Fig. 8. Nonetheless, there are a number of distinctive features in microlensing light curves which are hard to explain as intrinsic variations in luminosity. Perhaps the most characteristic feature of a microlensing amplification of a quasar accretion disc source with a radial colour gradient is the initial brightening in the red light curve as the red outer part of the accretion disc becomes amplified. This is then followed by a sharper increase in blue light and as the complex structure of the caustic is crossed, the features are seen to be smoothed out in red light. As the source leaves the caustic the process is reversed, with the blue light declining more quickly than the red, which persists for longer as the outer red part of the accretion disc is finally crossed. This is well illustrated in two quasar light curves from the Field 287 sample illustrated in Fig. 10, which show all the features of a complex caustic crossing.

The structure of the light curves in Fig. 10 raises another interesting question. Although they are clearly not symmetrical in time, from a statistical perspective microlensing amplification has no arrow of time. It is thus to be expected that for any particular photometric passband the timescales of increasing and decreasing light will

be the same. This question of statistical symmetry which has been discussed in general terms in Section 3 can be addressed by comparing histograms of yearly increases and decreases in magnitude. The expectation for the structure of these histograms of magnitude differences in quasar light curves on the basis that the variations are the result of microlensing can be addressed by computer simulations. The results are illustrated in Fig. 11 which is based on a sample of light curves from microlensing simulations similar to those illustrated in Fig. 8. Here, the blue line is a histogram of yearly magnitude increases, and the red line shows a similar histogram for yearly decreases in magnitude. It can be seen that there is no significant difference between the two histogram, as expected from the geometrical origin of the variations, and no statistical difference between the distribution of increasing and decreasing variations. The result of applying this test to the light curves of the Field 287 sample of quasars is shown in the top panel of Fig. 12. Again, there is no significant difference between the two histograms, consistent with the expectations for microlensing amplifications. Similar histograms for red light show the same effect, although histograms for red and blue light do not have the same structure, as illustrated in the bottom panel of Fig. 12.

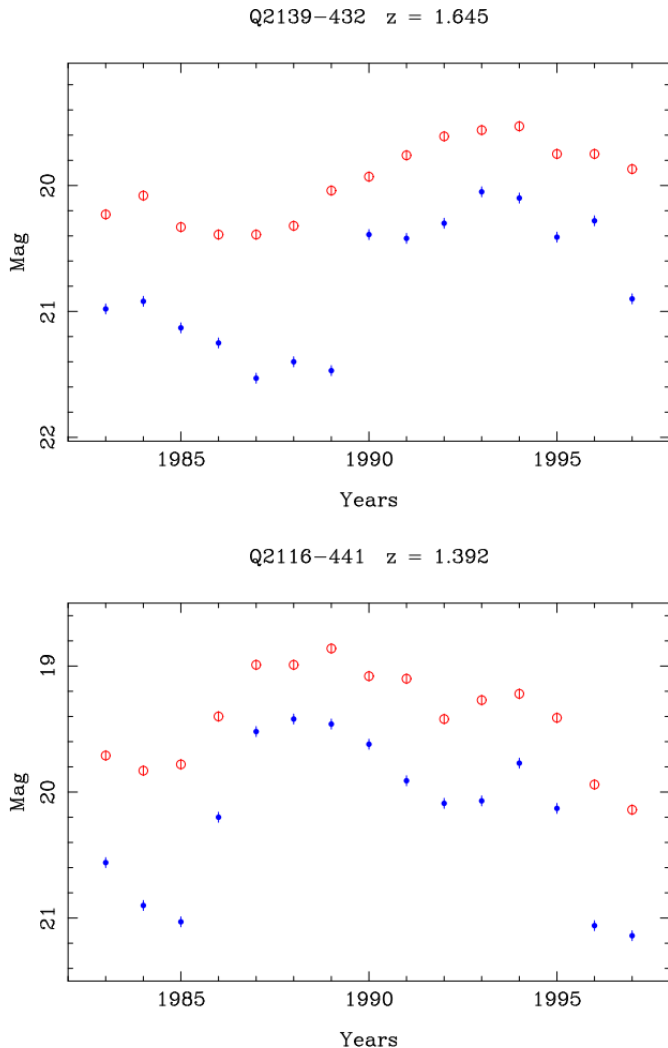


**Figure 10.** Two light curves from the Field 287 survey showing all the expected features of a complex caustic crossing. Symbols are as defined for Fig. 5.

The statistical symmetry of the quasar light curves as illustrated in Fig. 12 can be used as a further consistency check for the origin of the variations in quasar light. In fact, symmetry in quasar light curves has received little attention in the literature. The issue is discussed by Kawaguchi et al. (1998) in the context of disc instability models of quasar variation where they point out that in these models a slow rise in luminosity is followed by a rapid decline. They contrast this to a starburst model where a central disturbance propagates through the disc resulting in a rapid rise in luminosity, which is then followed by a more gradual decline, as might be seen in a supernova for example. The symmetry illustrated in the top panel of Fig. 12 implies that the observed quasar variations are not associated with models of this type, although it is possible that the two modes of variation could combine to give the appearance of symmetry. In fact it appears that microlensing is the only well-studied physically motivated model of quasar variation which predicts statistical symmetry in the light curves. It is however important to emphasise that the observed statistical symmetry in no way demonstrates that the quasar variations are the result of microlensing. It is perfectly possible that some as yet unidentified mode of variation in the accretion disc is responsible for

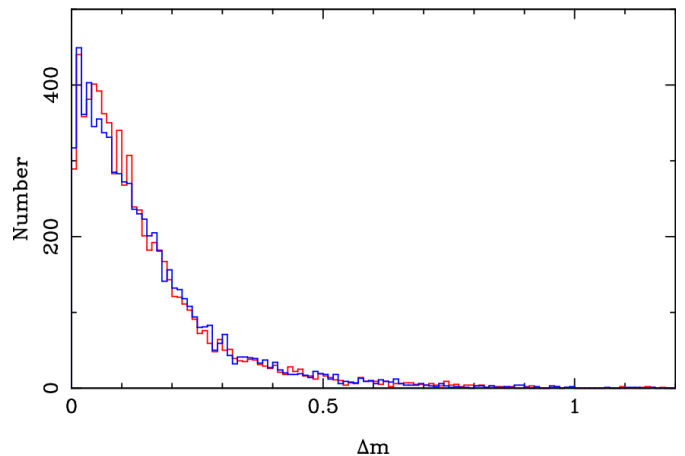


**Figure 11.** Histograms of yearly changes in magnitude in bins of 0.01 mag for light curves from computer simulations of microlensing amplifications. Blue and red histograms are for brightening and faintening changes in magnitude respectively.

the observed variability. The significance for the results of this paper is just that the symmetry observed in Fig. 12 is consistent with the predictions of microlensing.

The characteristic initial gentle increase in red light followed by a sharper increase in blue light can form a useful diagnostic for microlensing amplifications of an accretion disc with a temperature or colour gradient. The sample of quasar light curves in Stripe 82 provides a source for the identification of this mode of variation, and Fig. 13 illustrates four examples. Although the structure of the light curves can be quite complex, all four show an early slow increase in red light followed by a more rapid and larger rise in blue light. The short time coverage and uneven sampling of the Stripe 82 light curves unfortunately obscures the full range of the caustic crossings.

## 5 DISCUSSION

The idea behind this paper is to test the prediction that if stellar mass primordial black holes make up a significant fraction of the dark matter, then the resulting optical depth to microlensing on a cosmological scale will be sufficient to create a caustic web which when traversed by a quasar accretion disc will result in characteristic caustic crossing events in the quasar light curve. For low redshift nearby sources any microlensing events will be isolated and rare, and take the well-known form of a bell-shaped Paczyński profile. Such a feature in a quasar light curve would be hard to identify unambiguously, and would not provide an adequate test for the presence of lenses in the form of primordial black holes. However, in a  $\Lambda$ CDM universe caustics start to form at around an optical depth  $\tau \sim 0.1$  corresponding to a redshift  $z \sim 1.3$ , leading to non-linear amplification of the quasar light and characteristic structures in the quasar light curves.

Much of this paper has been devoted towards identifying features in quasar light curves which are consistent with the trajectory of the quasar across a web of caustics generated by a cosmological distribution of stellar mass lenses. In this context it is worth considering modes of intrinsic variation which might mimic microlensing. An important recent development in the understanding of quasar structure has been reverberation mapping of quasar accretion discs (Mudd



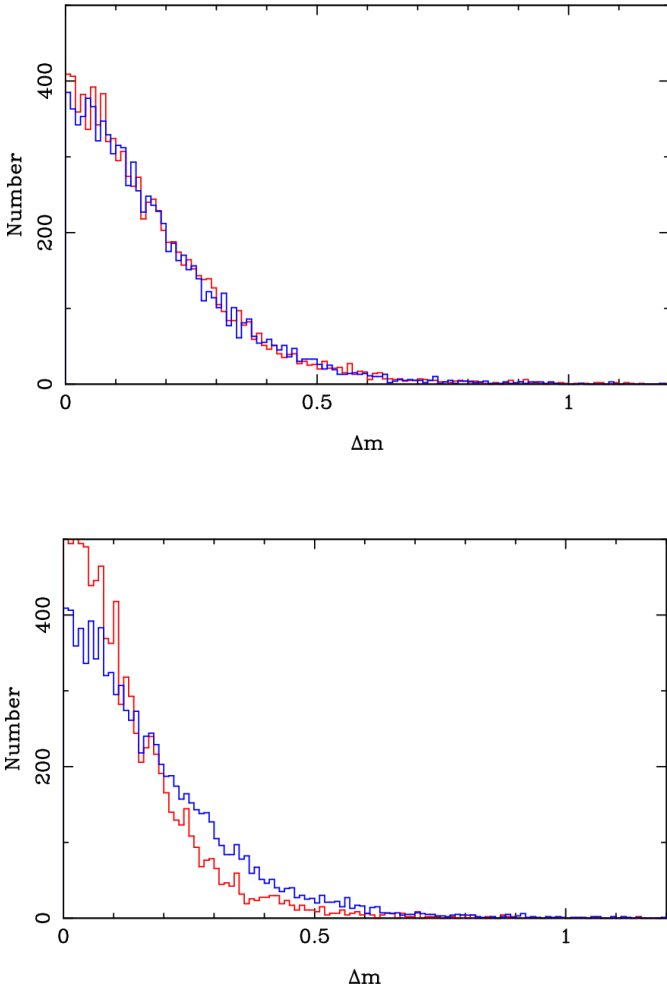


**Figure 12.** Histograms of yearly changes in magnitude in bins of 0.01 mag for the Field 287 quasar sample. The top panel shows brightening (blue histogram) compared with faintening (red histogram) changes for the blue passband light curves. The bottom panel shows brightening in the blue passband (blue histogram) compared with brightening in the red passband (red histogram).

et al. 2018). This technique is based on a model of quasar variability from Cackett et al. (2007) where central disturbances in the nucleus are reprocessed and propagated through an accretion disc where the temperature gradient is reflected in a matching colour gradient. The procedure adopted by Mudd et al. (2018) is to use the time lag between the arrival of the central disturbance in different photometric passbands to measure the size of the accretion disc. The typical time lags are measured to be a few days, roughly corresponding to light travel time between the colour zones in the disc, with variations in the red lagging behind those in the blue. This mode of variation would appear to be at odds with the analysis of quasar light curves from Field 287 and Stripe 82 samples. As can be seen in Fig. 13, time lags between photometric passbands are typically of the order of a year, and are almost always characterised by brightening in the red followed by more rapid brightening in the blue. This seems to be a different mechanism to the intrinsic changes observed in reverberation mapping projects.

The light curves containing candidate caustic crossing events illustrated in this paper should be seen as the identification of typical microlensing structures rather than a statistically meaningful sample. Although ideally such a search procedure would be implemented with an objectively defined algorithm, it became clear that the target light curves contained too many ill-defined parameters for this to be feasible. However, as the idea was to investigate the possibility that such candidate caustic crossing events were present in the data at all, a careful visual inspection of each multicolour light curve turned out to give very good results. The two surveys which were used to identify the microlensing events were significantly different in composition. The main strength of the Field 287 survey was the 26 year length of the light curves with uniform uninterrupted yearly observations. This fitted in well with the characteristic timescale of 10 to 20 years for caustic crossing events (Hawkins 2007). By contrast, the Stripe 82 survey is made up of light curves mostly covering 8 years, but in many cases with missing epochs. Its two great advantages are the 10,000 light curves it contains, in contrast to 1000 for the Field 287 sample, and the five photometric passbands of  $u$ ,  $g$ ,  $r$ ,  $i$  and  $z$  as opposed to just  $B_J$  and  $R$  for Field 287.

Although the search for caustic crossing events is not in any way complete, there are aspects of microlensing which can be tested statistically, and which can rule out modes of intrinsic changes in the luminosity of the accretion disc. The histogram in the top panel of Fig. 12 is based on the statistics of increasing and decreasing yearly magnitude increments for all 1033 quasars in the Field 287 sample. The strong symmetry between increasing and decreasing changes in magnitude puts tight constraints on the mechanism underlying the changes in quasar brightness. There have been a number of attempts to parametrise the variations seen in quasar light curves, notably as a damped random walk (DRW) process. This approach has been implemented by Kozłowski et al. (2010) who propose an exponential covariance matrix of the form

$$S_{ij} = \sigma^2 \exp(-|t_i - t_j|/\tau) \quad (2)$$

to model quasar light curves between epochs  $t_i$  and  $t_j$ , where  $\sigma$  defines the amplitude and  $\tau$  is the damping timescale. This formulation was then used by MacLeod et al. (2010) to model the time variability of quasars in the SDSS Stripe 82.

This parametrisation of the variations in quasar light curves is illustrated by the histogram in Fig. 14 using light curves generated by Eq. 2, which has a similar structure to those in the top panel of Fig. 12 and supports the idea that quasar light curve variations may be consistent with a DRW process (MacLeod et al. 2010). This parametrisation of the variations as statistically symmetric, combined with the observational evidence in Fig. 12 puts strong constraints on any physically motivated model of quasar variability, and is inconsistent with the disc instability and starburst models discussed in Section 4. Although there may be some room for asymmetry on short timescales  $\lesssim 1$  year, the expectation for a DRW process is that the magnitude variations will be symmetric in time. Given the complex physical structure of an accretion disc it is perhaps not surprising that models predicting symmetric variations in luminosity are not prominent in the literature. However, the more geometric nature of microlensing variations avoid most of these problems and would appear to provide a satisfactory model for the observed symmetry of variation, although intrinsic modes of variation cannot be ruled out.

There is still no clear consensus on the nature of a physically motivated model for intrinsic variations in quasar light on a timescale of years. The starburst model of Terlevich et al. (1992) was taken seriously when first published, but there has been little evidence to

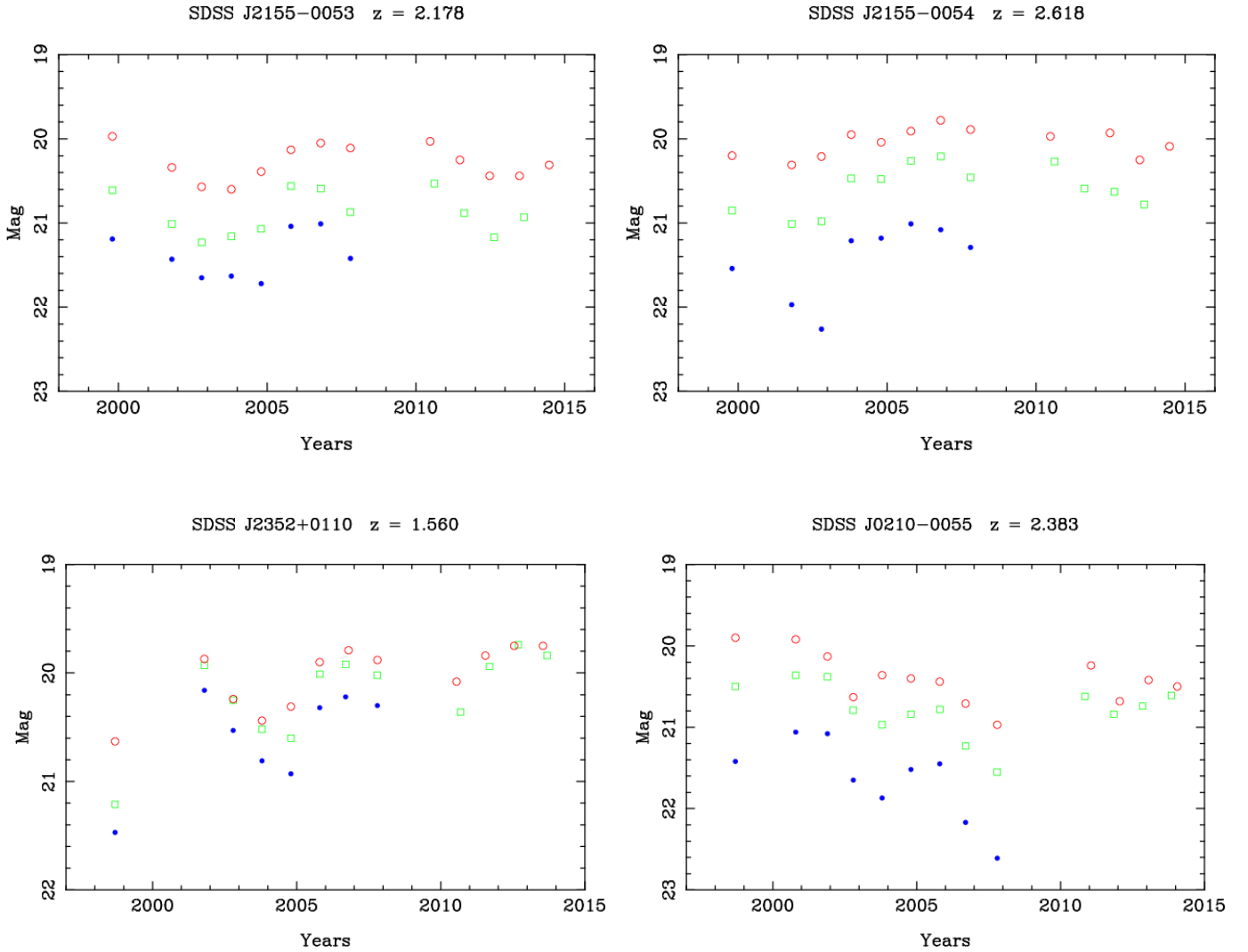


**Figure 13.** Quasar light curves from the SDSS Stripe 82 and Pan-STARRS1 data archives illustrating initial brightening in the red. Symbols are as for Fig. 7.

support it since then. The thermal reprocessing model of [Cackett et al. \(2007\)](#), developed by [Mudd et al. \(2018\)](#), seems to work well for accretion disc variations on timescales of days, but does not seem to be applicable on longer timescales. A promising mode of accretion disc variability proposed by [Mineshige et al. \(1994\)](#) and developed by [Takeuchi et al. \(1995\)](#) produces variations on the accretion timescale from a self organizing accretion disc. In this model accretion causes matter to build up in the accretion disc, moving towards the centre in a series of avalanches of various sizes. Using the description given by [Mineshige et al. \(1994\)](#) to simulate the self organizing accretion disc, a typical light curve generated by this process is shown in Fig. 15, and Fig. 16 shows histograms for brightening and faintening changes in luminosity for a large sample of simulated light curves. It can be seen that the two histograms are quite different, with the brightening changes largely confined to many small increases as material slowly accretes onto the disc, whereas the disc becomes fainter in much larger jumps as debris periodically cascades into the centre.

A further insight into quasar variability mechanisms can be obtained by considering the symmetry of variations in accretion discs with a significant colour gradient. The bottom panel of Fig. 12 shows

histograms of yearly brightening magnitudes for blue and red pass-band light curves, where the red histogram has been normalised to the blue numbers to take account of the smaller number of complete red passband light curves. Similar histograms for faintening magnitudes show the same structure. It will be seen that relatively speaking the blue light changes by larger increments than the red. In a disc with a colour gradient from blue in the centre changing to red in the outer parts this would favour models where a central disturbance in the blue part of the disc propagates outwards and decays towards the redder outer area. In disc instability models, a disturbance in the outer part of the disc, caused perhaps by infalling debris, results in a red flare followed by a confused response as the disturbance propagates through the remainder of the disc. It would appear that models of this type are not favoured by the histograms in the bottom panel of Fig. 12.

The expectation for the statistics of microlensing variations is closer to the central disturbance model rather than disc instability, as the central blue compact core will be more strongly microlensed than the more diffuse outer parts of the accretion disc. There will however be a significant difference in the timewise structure of the

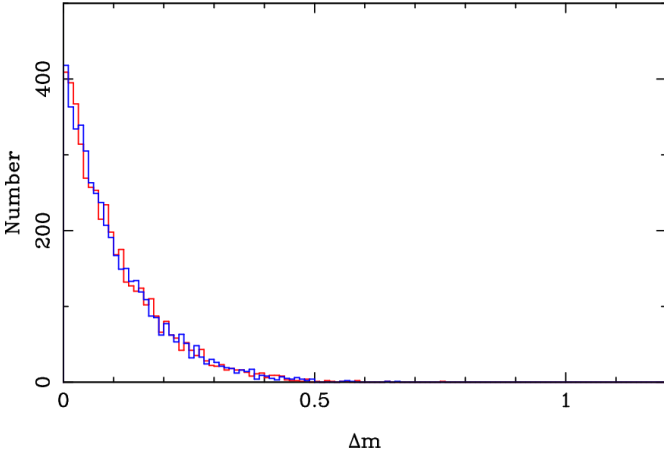


**Figure 14.** Histograms of yearly changes in magnitude in bins of 0.01 mag for light curves from computer simulations of variations from a damped random walk process. Blue and red histograms are for brightening and faintening changes in magnitude respectively.

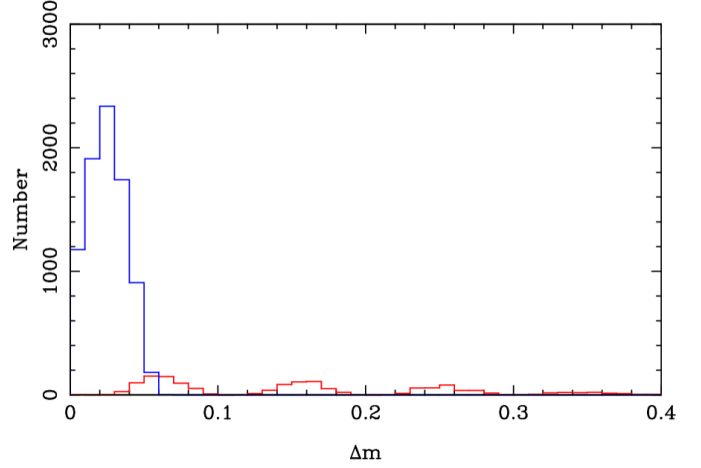


**Figure 16.** Histograms of changes in magnitude for a sample of light curves generated from the self organizing accretion disc model. Blue and red histograms are for brightening and faintening changes in magnitude respectively.

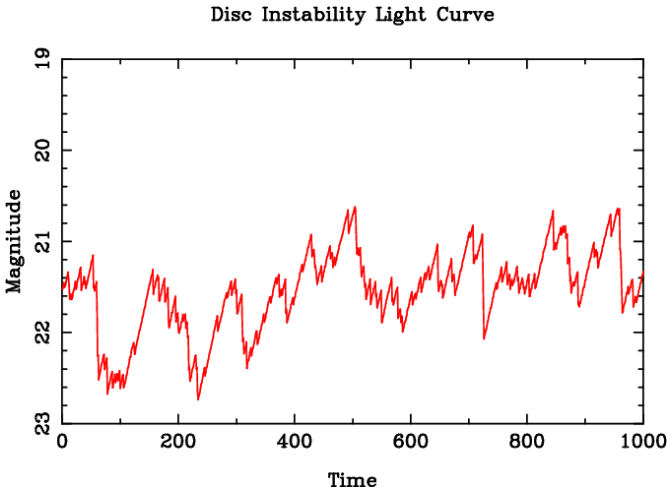


**Figure 15.** An example of a light curve generated by the self organizing accretion disc model, with arbitrary units of time and magnitude.

light curves. Microlensing will tend to produce an initial but relatively gentle rise in the red, as the large diffuse area of red light starts to be microlensed. This will be followed by a much sharper rise in blue light as the compact blue nucleus is microlensed. This mode of variation is very distinctive, and is indeed a feature of the simple caustic crossing simulated in Figs 3 and 4.

The bottom panel of Fig. 12 illustrates another little discussed statistical feature of colour changes in quasar light curves. The rapid rises and falls in blue light compared with the red light has a geometrical explanation illustrated in Fig 4, with observational examples in Figs 6 and 7. It is hard to imagine a mode of variation in accretion disc light which could mimic this, and certainly no currently discussed accretion disc model has these properties. This includes the time lags in reverberation mapping measurements which are typically on

the order of a few days and are quite distinct from caustic crossing events.

It is important to point out that these chromatic effects will only be seen in quasar light curves when the visible part of the accretion disc is larger than the Einstein radius of the lens. Otherwise, any colour gradient will not be resolved, and variations in light due to microlensing will be achromatic. This is consistent with observations of quasar light curves which are largely characterised by achromatic variations.

## 6 CONCLUSIONS

The idea behind this paper has been to test the proposal that stellar mass primordial black holes make up a significant fraction of the dark matter by looking for evidence of caustic crossings in quasar light curves. The first part of the paper uses microlensing simulations to define the expected features in quasar light curves produced by a cosmological distribution of stellar mass primordial black holes making up the dark matter. These features are distinctive, and are not easily confused with modes of variation in accretion disc luminosity. The features in quasar light curves which are associated with microlensing include the characteristic cuspy structures resulting from caustic crossings and the gradual rise in brightness in the red, followed by a sharper rise in the blue as the colour gradient in an accretion disc is traversed by a microlens. In addition, the statistics of yearly increase and decrease of brightness in quasar light curves is symmetrical, as expected from the geometrical nature of gravitational lensing. The case is made that this is not a property shared by current models of changes in accretion disc luminosity. These observations do not necessarily mean that all quasar variability is caused by microlensing, but that if a substantial fraction of dark matter is in the form of stellar mass primordial black, then the expected microlensing features in quasar light curves are actually observed.

**DATA AVAILABILITY**

The data upon which this paper is based are all publicly available and are referenced in the text, with footnotes to indicate online archives where appropriate.

**REFERENCES**

- Alcock C. et al., 1996, *ApJ*, 461, 84  
 Alcock C. et al., 2000, *ApJ*, 542, 281  
 Bate N.F. et al., 2018, *MNRAS*, 479, 4796  
 Byrnes C.T., Hindmarsh M., Young S., Hawkins M.R.S., 2018, *JCAP*, 08, 041  
 Cackett E.M., Horne K., Winkler H., 2007, *MNRAS*, 380, 669  
 Calcino J., García-Bellido J., Davis T.M., 2018, *MNRAS*, 479, 2889  
 Carr B., Clesse S., García-Bellido J., Kühnel F., 2021, *Phys. Dark Univ.*, 31, 100755  
 Carr B., Clesse S., García-Bellido J., Hawkins M.R.S., Kühnel F., 2024, *Phys. Rept.*, 1054, 1  
 Fukugita M., Futamase T., Kasai M., Turner E., 1992, *ApJ*, 393, 3  
 García-Bellido J., Hawkins M.R.S., 2024, *Universe*, 10, 449  
 Givon U., Maoz D., Kaspi S., Netzer H., Smith P.S., 1999, *MNRAS*, 306, 637  
 Hambly N.C., Irwin M.J., MacGillivray H.T., 2001, *MNRAS*, 326, 1295  
 Hawkins M.R.S., 1996, *MNRAS*, 278, 787  
 Hawkins M.R.S., 1998, *A&A*, 340, L23  
 Hawkins M.R.S., 2007, *A&A*, 462, 581  
 Hawkins M.R.S., 2010, *MNRAS*, 405, 1940  
 Hawkins M.R.S., 2015, *A&A*, 575, A107  
 Hawkins M.R.S., 2020a, *A&A*, 633, A107  
 Hawkins M.R.S., 2020b, *A&A*, 643, A10  
 Hawkins M.R.S., 2022, *MNRAS*, 512, 5706  
 Hawkins M.R.S., 2024, *MNRAS*, 527, 2393  
 Jiao Y. et al., 2023, *A&A*, 678, A208  
 Kawaguchi T., Mineshige S., Umemura M., Turner E.L., 1998, *ApJ*, 504, 671  
 Kayser R., Refsdal S., Stabell R. 1986, *A&A*, 166, 36  
 Kofman L., Kaiser N., Lee M.H., Babul A., 1997, *ApJ*, 489, 508  
 Kozłowski S. et al., 2010, *ApJ*, 708, 927  
 Lewis G.F., Brewer B.J., 2023, *Nat. Astron.*, 7, 1265  
 Luo Y., Shen Y., Yang Q., 2020, *MNRAS*, 494, 3686  
 MacLeod C. et al., 2010, *ApJ*, 721, 1014  
 MacLeod C. et al., 2012, *ApJ*, 753, 106  
 Matthews T.A., Sandage A.R., 1963, *ApJ*, 138, 30  
 Mediavilla E. et al., 2009, *ApJ*, 706, 1451  
 Mineshige S., Ouchi B.N., Nishimori H., 1994, *PASJ*, 46, 97  
 Mudd D. et al., 2018, *ApJ*, 862, 123  
 Neira F., Anguita T., Vernados G., 2020, *MNRAS*, 495, 544  
 O'Hare C.A.J., 2021, *Phys. Rev. Lett.*, 127, 251802  
 Ou X., Eilers A.-C., Necib L., Frebel A., 2024, *MNRAS*, 528, 693  
 Paczyński B., 1986, *ApJ*, 304, 1  
 Peterson B.M., 1993, *PASP*, 105, 247  
 Pooley D., Rappaport S., Blackburne J. A., Schechter P.L., Wambsganss J., 2012, *ApJ*, 744, 111  
 Refsdal S., Stabell R., 1991, *A&A*, 250, 62  
 Schneider P., Weiss A., 1986, *A&A*, 164, 237  
 Schneider P., Ehlers J., Falco E.E., 1992, *Gravitational Lenses*, Springer: New York  
 Stone Z. et al., 2022, *MNRAS*, 514, 164  
 Takeuchi M., Mineshige S., Negoro H., 1995, *PASJ*, 47, 617  
 Terlevich R., Tenorio-Tagle G., Franco J., Melnick J., 1992, *MNRAS*, 255, 713  
 Vernados G. et al., 2024, *Space Sci. Rev.*, 220, 14  
 Wambsganss J., 1999, *JCoAM*, 109, 353

This paper has been typeset from a  $\text{\LaTeX}$  file prepared by the author.